

Detecting Path Anomalies in Time Series Data on Networks

Timothy LaRock
Network Science Institute
Northeastern University
Boston, MA, USA

Vahan Nanumyan
Chair of Systems Design
ETH Zürich
Zürich, Switzerland

Tina Eliassi-Rad
Network Science Institute
Northeastern University
Boston, MA, USA

Ingo Scholtes
Data Analytics Group
University of Zurich
Zürich, Switzerland

Giona Casiraghi
Chair of Systems Design
ETH Zürich
Zürich, Switzerland

Frank Schweitzer
Chair of Systems Design
ETH Zürich
Zürich, Switzerland

ABSTRACT

The unsupervised detection of anomalies in time series data has important applications, e.g., in user behavioural modelling, fraud detection, and cybersecurity. Anomaly detection has been extensively studied in categorical sequences. But we often have access to time series data that contain *paths* in networks. Examples include transaction sequences in financial networks, click streams of users in networks of cross-referenced documents, or travel itineraries in transportation networks. To reliably detect anomalies we must account for the fact that such data contain a large number of independent observations of short paths constrained by a graph topology. Moreover, the heterogeneity of real systems rules out frequency-based anomaly detection techniques, which do not account for highly skewed edge and degree statistics. To address this problem we introduce HYP A, a novel framework for the unsupervised detection of anomalies in large corpora of variable-length temporal paths in a graph. HYP A provides an efficient analytical method to detect paths with anomalous frequencies that result from nodes being traversed in unexpected chronological order.

1 INTRODUCTION

Anomaly detection refers to the problem of finding “patterns in data that do not conform to a well defined notion of normal behaviour,” [16]. The importance of anomaly detection techniques rests on the fact that such anomalous patterns may carry important meaning. Examples include anomalous usage or traffic patterns used to detect cyberattacks, anomalous sensor readings that may identify imminent faults in technical systems, or anomalous transactions patterns used to detect fraud and compliance violations in financial systems. In order to assess which data represent “anomalies”, we must define what we consider “normal behaviour” in the particular system under study. Given this baseline of “normal behaviour”, we must develop methods to efficiently assess which instances in the data exhibit deviations from this baseline. Lastly, we need techniques to argue which of those observed deviations are *significant* given the fluctuations and randomness contained in data.

While the anomaly detection problem has been studied extensively for general categorical sequence data, we are often confronted with time series data capturing *paths through networks*. Such data have special characteristics. Different from general categorical sequences, an underlying graph topology constrains which paths, i.e., sequences of node traversals, can possibly occur. Moreover, the

graphs in which paths are observed often exhibit strong heterogeneities, e.g., heavily skewed node degree distributions or heterogeneous edge statistics. These heterogeneities invalidate frequency-based anomaly detection techniques that do not account for the fact that in real systems some paths are more likely to be observed at random than others (see example in Fig. 1).

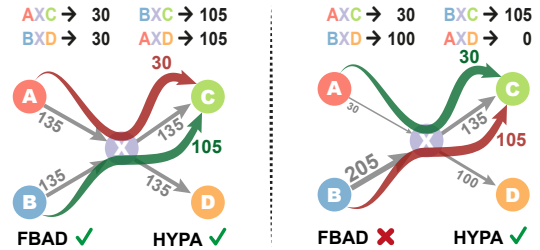


Figure 1: Frequency-based anomaly detection (FBAD) can be used to identify ground truth under- (red) and over-represented (green) paths in graph with homogenous edge statistics (left), but fails to identify anomalies in data with heterogeneous edge statistics (right). Our proposed method HYP A succeeds in both scenarios. For illustrative purposes, the example only contains paths of length $k = 2$, while HYP A detects anomalies at any length k in variable-length data.

Closing this gap, we consider the problem of detecting *anomalous paths* in heterogeneous graphs based on large time series data capturing sequences of node traversals. Our definition of *anomalous paths* is based on a memoryless baseline model, which assumes that the chronological order of node traversals is uniquely determined by the graph topology and the statistics of edge traversals. Our method, HYP A thus detects anomalous paths consisting of nodes with unexpected temporal traversal patterns.

This problem is of practical relevance in a number of scenarios. For a graph capturing hyperlinks between web pages, we can consider a set of click streams generated by users navigating the pages. Here, anomalous paths between Web pages could translate to semantic similarities or differences that lead users to navigate links in this specific order more or less often than expected at random. Similarly, for data containing sequences of transactions between actors in a financial network, path anomalies signify frequent paths of money exchange across subsets of financial actors. And for trajectories of passengers on flights through the network of US airports,

anomalous paths convey information about the role of airports in routing flights through the country.

To support such studies we propose HYPAs, a novel method for unsupervised anomaly detection in collections of variable-length sequences capturing paths in a graph. Our main contributions are:

- (i) We introduce the problem of detecting *path anomalies*, referring to paths in a graph that occur more or less often than expected under a random null model. We further show that the problem of detecting *anomalous paths* of length k can be reduced to the problem of detecting *anomalous edges* in a k -dimensional De Bruijn graph model of paths in a graph.
- (ii) We use an analytically tractable statistical model of random, weighted De Bruijn graphs to derive closed-form expressions for the cumulative weight distribution of paths of any length k observed in data. We introduce HYPAs, a path anomaly detection algorithm that leverages these weight distributions to detect paths that occur significantly more or less often than expected at random. Anomalies are identified based on a discrimination threshold, which can be set either heuristically or according to a p -value of a hypothesis test.
- (iii) We validate HYPAs in synthetic data with known anomalies introduced for different path lengths. The results show that HYPAs detects anomalies at the correct order k with high accuracy. The applications of HYPAs to empirical data on user trajectories in transportation and information systems show that the detected anomalies can be validated using geographical or semantic information.

Providing a novel scalable method for the unsupervised detection of anomalies that is grounded in graph theory and statistical modeling, our work opens new opportunities for the mining of patterns in time series data on networks. The runtime of HYPAs scales linearly with the size of the data, making it suitable for big data scenarios.

2 RELATED WORK AND BACKGROUND

Before introducing our method, we first summarize related works on anomaly detection and sequential pattern mining. We further provide the background of higher-order graph models and statistical graph ensembles underlying our method.

2.1 Related Work

Considering the large body of research on anomaly detection in time series data [24], and keeping in mind the focus of this paper, we limit our review to related works on (i) anomaly detection in discrete sequences, (ii) sequential pattern mining, and (iii) graph-based anomaly detection. Since we are concerned with the unsupervised detection of path anomalies we further exclude (semi-)supervised and reinforcement learning techniques.

Anomaly Detection in Sequence Data. Following [17, 18], anomaly detection techniques for discrete sequences fall into different categories that address fundamentally different application scenarios. Sequence-based anomaly detection assumes that we are given a set $S = \{s_1, s_2, \dots, s_n\}$ of sequences $s_i = (x_j)_{j=1, \dots, l_i}$ over a discrete alphabet Σ , possibly with variable lengths l_i . One then considers the problem of finding anomalous instances s_i in S , e.g., by assigning an anomaly score to each sequence in the database.

For instance, if the sequences s_i capture sensor readings of different machines or system call sequences in user sessions on a computer, these anomalies can tell us which machines are likely to experience imminent failures or which user accounts have likely been hijacked by an intruder. Different approaches have been used to establish a random baseline against which sequences are defined as “anomalous”. Some works use (hidden) Markov chain models, e.g., to detect (groups of) sequences which show significant differences in terms of state transition probabilities [4, 29, 31, 45]. Other methods use nearest-neighbours algorithms [32] or distance measures [47] to quantify how any given sequence s_j differs from other instances in S . Adopting a collective definition of anomalies [16], a third class of methods is based on hypothesis testing techniques to detect outliers in the distribution of features of sequences [5, 30, 46].

Sequential pattern mining. A common feature of the works above is that they focus on anomalies at the level of a whole sequence s_j within S . Addressing a different problem, a number of works instead consider the problem of finding anomalous *patterns* or *subsequences* within a long sequence $S = (x_i)_{i=1, \dots, n}$ [17]. This is closely related to sequential pattern mining [1], e.g., algorithms to quickly find the most frequent subsequences in large sequence data [20, 43]. Other works address this problem based on statistical methods, e.g., using Markov modelling techniques [12, 25, 37, 39, 50, 53], hypothesis testing [8, 44], or information-theoretic methods to detect “surprising” subsequences [9, 15, 27]. Applications include the detection of common patterns in user trajectories [38, 50], testing hypotheses about generative processes of trajectory data [44], or finding clusters in click streams and other sequence data [12, 37].

Temporal Anomaly Detection in Graphs. Compared to the problem of anomaly detection in general discrete sequences addressed in the works above, the problem motivating our method is different in multiple ways. First and foremost, the methods above make no assumptions about the relational structure of data, while we consider *sequential data capturing paths in a (weighted and directed) graph topology*. This aligns our work more closely to anomaly detection techniques for temporal graph data that have been developed in the graph mining community [3, 35]. As summarized in [3, 10] these works mainly study the detection of change events [2] or cluster structures in evolving graphs [11, 37]. Different from these problems, our method uses a set S of sequences – capturing, e.g., click streams in a hyperlink graph, humans travelling in a transportation network, or communication sequences in a social network – to identify paths of nodes that are traversed more or less often than expected. Hence, rather than making statements about anomalous instances in S , we use collective statistical information in S to identify sequences of nodes traversed with *anomalous frequencies*.

2.2 Background

Due to the growing volume of time series data capturing *trajectories* or *paths* in networked systems, the modeling of patterns in these data has become the focus of recent works in graph mining and network science. Addressing the detection of exceptional trajectories, previous work [4, 6] develops a framework that can be used to test hypotheses about generative processes. A number of recent works use higher-, variable-, and multi-order models of paths in order to detect, model and quantify deviations from the Markovian expectation [28, 36, 38, 40–42, 52]. Contributing to this line of research, our

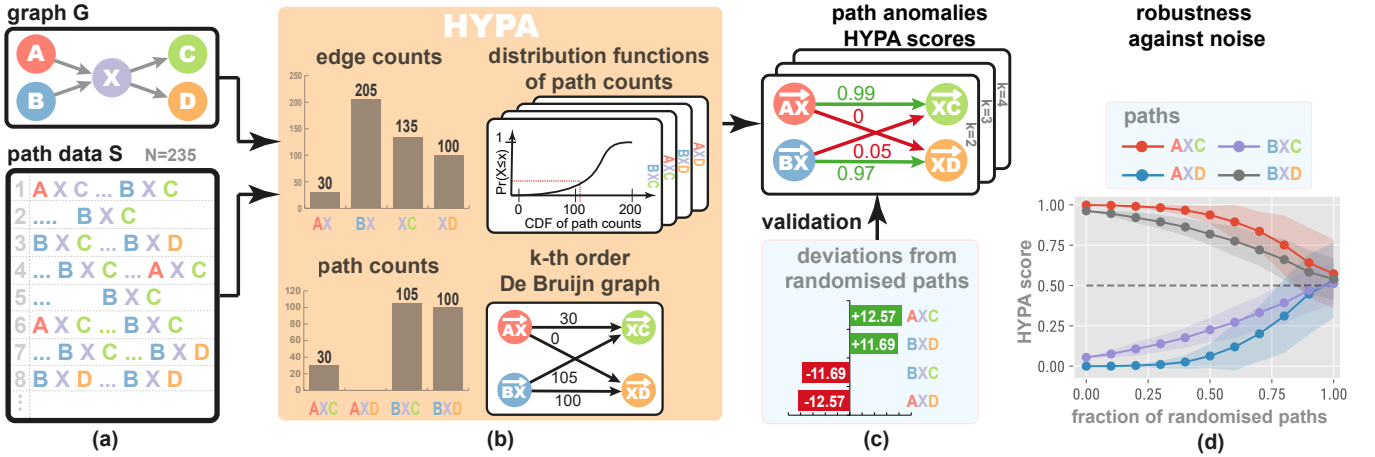


Figure 2: A toy example of path data S observed in a graph G illustrates path anomaly detection with HYPA (focusing on $k=2$). Given a set of sequences traversing nodes $A, B, X, C,$ and D in a graph (a), HYPA uses higher-order De Bruijn graphs to derive closed-form expressions for the cumulative distribution function of all possible paths in the graph (b). HYPA computes HYPA-scores (c) that allow reliable detection of over- and under-represented paths, even in situations where the least frequent path (AXC) is over-represented, while the most frequent path (BXC) is under-represented. Progressive randomization of the data gradually levels HYPA-scores (d), translating to a decreasing confidence at which we detect path anomalies.

work provides a new foundation for the efficient detection of path anomalies in time series data on graphs. Our method specifically overcomes complications in the reliable detection of significant path anomalies in directed and weighted graphs, which (i) have not been addressed in the graph mining and sequence mining literature, and (ii) rule out applications of common frequency-based methods to detect collective anomalies.

Contributing to recent research on higher-order graph models [28], our method is based on a projection that reduces the problem of detecting anomalous *paths* in a (first-order) graph model to the problem of detecting anomalous *edges* in *higher-order* graph models that resemble De Bruijn graphs [19]. Similar to [41], we define a higher-order De Bruijn graph model of paths as follows:

Definition 2.1 (k -th order De Bruijn graph model of paths).

For a given graph $G = (V, E)$ and $k \in \mathbb{N}$ we define a k -th order De Bruijn graph of paths in G as a graph $G^k = (V^k, E^k)$, where (i) each node $\vec{v} := v_0 v_1 \dots v_{k-1} \in V^k$ is a path of length¹ $k - 1$ in G , and (ii) $(\vec{v}, \vec{w}) \in E^k$ iff $v_{i+1} = w_i$ for $i = 0, \dots, k - 2$.

This definition has several implications. First, any two nodes \vec{v} and \vec{w} connected by an edge in a k -th order graph G^k represent two paths of length $k - 1$ that overlap in exactly $k - 1$ out of k nodes. Since paths in a graph are transitive, each edge (\vec{v}, \vec{w}) in G^k represents a path of length k in graph G . This implies that the graph G itself is a first-order De Bruijn graph of paths of length one (i.e., edges) in G i.e., $G^1 = G$. We can see De Bruijn graphs as generalization of standard, first-order graphs to higher-order models of paths of length k , where any path of length q in G^k translates to a path of length $k + q - 1$ in G . We iteratively construct such De Bruijn graph models of order k by means of a line graph transformation of the De Bruijn graph model of order $k - 1$.

¹We assume that path length counts the number of edges traversed in G

The benefit of this representation is that it allows us to represent the frequencies of paths of length k observed in a graph to the weights of edges in a k -th order De Bruijn graph. This can be seen in the illustration of a De Bruijn graph with order $k = 2$ in Fig. 2, where nodes represent paths of length $k - 1 = 1$ (i.e., edges in G) that overlap in $k - 1 = 1$ nodes, while edges represent all paths of length $k = 2$. Note that we also consider all *subpaths of length two*, i.e., paths of length two contained in longer paths.

This simple higher-dimensional projection of paths in a graph allows us to reduce the problem of detecting paths of length k that exhibit anomalous frequencies to the problem of detecting anomalous edge weights in a k -th order De Bruijn graph. To understand which edge weights exhibit “anomalies”, we need a suitable null model that provides the baseline against which we want to compare the observed weights. We specifically need a way to generate randomized configurations of the path data that selectively destroy those patterns that we are interested in, while preserving all other characteristics. Thanks to the projection of paths to edges of a directed and weighted (De Bruijn) graph, we can address this problem by employing *statistical graph ensembles*, which randomize certain aspects of a graph (i.e., the weights of edges or the topology) while preserving other characteristics. Examples include simple models that randomize the topology of a given graph while preserving the (expected) number of edges [23], as well as combinatorial models that preserve the degrees of nodes [34].

An analytically tractable formulation of such a model for directed and weighted graphs was recently proposed in [13]. It treats the random generation of weighted graphs as an urn problem, where random edges are drawn without replacement from a population of multi-edges connecting different pairs of nodes. Through this formulation, the probability of generating edges with specific weights can be calculated based on the multivariate hypergeometric distribution. While this formulation can be used to detect anomalous edges in social networks [14], no analytically tractable null models

that account for the special characteristics of De Bruijn graphs, i.e., the fact that a directed edge between two nodes in a k -th order De Bruijn graph can only exist if the corresponding path exists in the underlying graph, have been proposed. Closing this gap, we present a novel method to detect path anomalies based on statistical ensembles of k -th order De Bruijn graph models.

3 HIGHER-ORDER HYPER-GEOMETRIC PATH ANOMALY DETECTION

We now define the problem of *path anomaly detection*, illustrate the problem in an example, and introduce our proposed solution.

Definition 3.1 (Path Anomaly Detection). Let $G = (V, E)$ be a directed graph and S a set of n sequences s_i , where each sequence $s_i = v_0 v_1 \dots v_{l_i}$ is a *path* of length l_i in G , i.e. $v_j \in V$ for $j \in [0, \dots, l_i]$ and $(v_j, v_{j+1}) \in E$ for $j \in [0, \dots, l_i - 1]$. For $k > 1$, identify all paths $\vec{p} = \vec{v}_0 \dots \vec{v}_k$ of length k in G whose frequencies, as subpaths, in S significantly deviate from the frequencies expected in a $(k - 1)$ -order model of paths in G .

We do not assume that the observed sequences have the same lengths l_i and we particularly consider data capturing many short paths. Unlike *sequence-based anomaly detection techniques* [17], we are not interested in assigning an *anomaly score* to each sequence s_i in S . We instead want to use the instances in S to identify which paths in the graph exhibit anomalous frequencies compared to a “random baseline”. Hence, rather than detecting anomalies in S , we use S to learn which paths in G are traversed in an anomalous fashion. To complete our definition of *anomalies*, we define a generative *null model* for paths that builds on definition 2.1. We use it to establish the baseline against which we detect anomalies [16].

Definition 3.2 (k -th order model of paths). For a graph G let $G^k = (V^k, E^k)$ be a k -th order De Bruijn graph of paths in G (cf. Def. 2.1). For each edge $e := (\vec{v}_0 \dots \vec{v}_{k-1}, \vec{v}_1 \dots \vec{v}_k) \in E^k$ let the weight $f(e)$ be the frequency of subpath $\vec{v}_0 \dots \vec{v}_k$ in S . Let \mathbf{T}^k be the transition matrix of an edge-weighted random walk on G^k , i.e., $\mathbf{T}^k_{\vec{v}, \vec{w}} := \frac{f(\vec{v}, \vec{w})}{\sum_{\vec{x} \in V^k} f(\vec{v}, \vec{x})}$. For a path $\vec{p} = \vec{v}_0 v_1 \dots v_l$ with $l \geq k$ the k -th order model of paths generates \vec{p} with probability $\prod_{i=k}^l \mathbf{T}^k_{\vec{v}_{i-k} \dots \vec{v}_{i-1}, \vec{v}_i \dots \vec{v}_{i+k-1}}$.

The model defined above generates paths of length l by performing $l - k + 1$ random walk steps in a k -th order De Bruijn graph. We can use such a model to generate random paths of length $l \geq k$ that respect (i) the topology of the underlying graph G , and (ii) the frequencies of paths of length k observed in S .

Our definition of path anomalies of length k is based on a null model of order $k - 1$. For $k = 2$, the null model of order $(k - 1) = 1$ is simply an edge-weighted random walk on the graph G . In this case, the sequence of nodes traversed by paths is *Markovian*, i.e., the node v_{i+1} on a path only depends on the current node v_i and the graph topology. Apart from the topology, the model accounts for the frequencies at which paths in S traverse edges in G . That is, if an edge (b, c) is traversed more often than (b, d) we expect path \vec{abc} to occur more often than \vec{abd} . For $k > 2$, the null model corresponds to an edge-weighted random walk on a De Bruijn graph of order $(k - 1) > 1$, where weighted edges capture the frequencies of subpaths of length $k - 1$ in S . This approach to generating a null

model is key to disentangling path anomalies that unfold at different lengths k : For any given length k it enables us to exclusively detect those path anomalies that do not trivially result from anomalous path frequencies at shorter lengths. In other words, to answer the question whether a *specific* path \vec{abcd} of length $k = 3$ is observed more or less often than expected, we discount for any anomalies of shorter paths \vec{abc} and \vec{bcd} contained in \vec{abcd} .

3.1 Illustrative Example

A simple example to illustrate the path anomaly detection problem for $k = 2$ is shown in Fig. 2, which gives a high level overview of our method HYP A. Limiting our focus to paths that traverse nodes A, B, X, C , and D , we consider a set S that contains 235 (sub)paths of length two. We observe strong heterogeneities in the path frequencies, where the most frequent path \vec{BXC} occurs 105 times, while the least frequent path \vec{AXC} occurs only 30 times.

Assume we want to detect for which paths of length $k = 2$ the frequencies deviate from the expectation in a first-order null model. If all paths were expected to occur with the same frequency, we could directly answer this question based on the distribution of path frequencies (cf. Fig. 1). Such an approach would trivially detect that path \vec{AXC} occurs more often than expected while path \vec{BXC} occurs less often than expected. However, the edge frequencies in our toy example show strong heterogeneities, where, for example, edge (B, X) is traversed about seven times more often than edge (A, X) (see Fig. 2). If we account for this heterogeneity of edges (i.e., paths of length $k - 1 = 1$), the question of which paths of length $k = 2$ exhibit statistically significant deviations becomes non-trivial. In particular, the same observed frequency f can be (i) “normal”, i.e., expected, for one path \vec{p}_1 , (ii) a significant over-representation for another \vec{p}_2 , and (iii) an under-representation for a third \vec{p}_3 .

We could address this problem by simulating the first-order model: we can randomly generate paths by means of a random walk model and then count their average frequencies across many simulations. A comparison of observed vs. average frequencies of paths of a given length k then indicates which paths exhibit deviations from the random baseline. In Fig. 2, we report the average of 100 such simulation runs, which indicate that paths \vec{AXC} and \vec{BXD} occur *more* often than expected, while paths \vec{BXC} and \vec{AXD} occur *less* often than expected. This simple example highlights an important problem. Due to the heterogeneous frequency of edges, paths that occur with the smallest frequency (\vec{AXC}) can actually be over-represented, while paths that occur with the highest frequency (\vec{BXC}) can be under-represented. This rules out collective anomaly detection techniques that assess anomalies based on a *single* frequency distribution.

We must instead consider the joint distribution of frequencies under the null model for each possible path and each length k separately. While a simulation-based approach is possible in principle, the combinatorial growth of the required computational effort for large systems is prohibitive. Moreover, such simulations leave open the question of whether the observed deviations in the data indicate a significant pattern or are likely due to chance. Projecting paths of length k onto edges in a k -dimensional De Bruijn graph, HYP A uses closed-form expressions for the cumulative distribution function of path frequencies under the $(k - 1)$ -order null model for each path

individually (see Fig. 2b). This enables us to analytically calculate *HYPAscores*, which, for each path \vec{p} , capture the likelihoods that a null model generates realizations where frequencies of \vec{p} are larger or smaller than in the data. The calculated HYPAscores can then be used to detect path anomalies at various levels of significance.

3.2 Hypergeometric Ensemble of Higher-Order De Bruijn Graphs

We now introduce the details of *higher-order hypergeometric path anomaly detection* (HYPA), the main contribution of our work.

Mapping of null model to ensemble of k -th order De Bruijn graphs. In the illustrative example, we showed that assessing whether a path of length k exhibits anomalous frequencies requires considering the distribution of frequencies under a null model *for each path separately*. The key idea of HYPAs is to map the difficult problem of finding the frequency distributions of paths of length k under a null model to the simpler problem of finding the edge weight distribution in a null model for k -th order De Bruijn graphs. For this, we remember that the weights on the edges in a k -th order De Bruijn graph can exactly represent the frequencies of paths of length k observed in a dataset (cf. Definition 3.2). We are thus interested in identifying which of these weights are anomalous compared to the baseline given by a $(k - 1)$ -order null model of paths. In each realization generated by such a $(k - 1)$ -order model, frequencies of paths of length $k - 1$ are fixed, while the frequency of each path of length k follows a different distribution that depends on the null model. We can map each random realization to a different weighted k -th order De Bruijn graph, obtaining a *statistical ensemble of k -th order De Bruijn graphs* whose probabilities are given by the null model. Since the frequencies of paths of length $k - 1$ are fixed, the *total* out-degree $f_{\vec{v}}^{\text{out}} = \sum_{\vec{x}} f(\vec{v}, \vec{x})$ and the *total* in-degree $f_{\vec{v}}^{\text{in}} = \sum_{\vec{x}} f(\vec{x}, \vec{v})$ for each node \vec{v} is the same across all realizations in this ensemble. However, De Bruijn graphs that correspond to different random realizations differ in terms of the exact edge weights $f(\vec{v}, \vec{w})$, which represent frequencies of paths of length k .

Distribution of edge weights in random k -th order graphs. Thanks to this mapping, we can find the frequency distributions of individual paths of length k conditional on the frequencies of paths of length $k - 1$ based on a random model for k -th order De Bruijn graphs. This model preserves the total in- and out-degrees of all nodes, while randomly shuffling the weights of edges. We can formalize the model as a stochastic process that randomly draws m edges, where m is the total number of (weighted) edges in the graph, i.e. the sum of all edge weights, which corresponds to the total number of paths of length k observed in the data. Different from simple random graph models, in this sampling process we must account for the fact that different edges in a k -th order De Bruijn graph have different probabilities to be drawn. Specifically, we are more likely to generate edges between pairs of nodes with a high in- and out-degree. In our null model of paths, this translates to the fact that a path of length k is more likely to occur if it continues a frequently occurring path of length $k - 1$. We capture the fact that different edges in a k -th order De Bruijn graph occur with different probabilities by means of a matrix Ξ . Each entry of this matrix corresponds

to one possible pair of nodes that can be connected by an edge, and the value of the entry denotes how many times this pair of nodes can possibly be drawn. We thus obtain a sampling procedure that can be described by the multivariate hypergeometric distribution.

Since we consider k -th order De Bruijn graphs we must additionally account for the fact only pairs of higher-order nodes representing paths overlapping in $k - 1$ first-order nodes can be connected (cf. Def. 2.1). When sampling from the multivariate hypergeometric distribution, we avoid drawing such pairs by setting their corresponding entry in Ξ to 0. This modification introduces the complication that weighted degrees are no longer guaranteed to be preserved, which violates the constraint that the frequency of paths of length $k - 1$ is fixed. We overcome this with an optimization approach (Algorithm 2 in Appendix A.1) that redistributes those values of the Ξ matrix that were substituted by zeroes across the rest of the matrix, such that the weighted degrees $f_{\vec{v}}^{\text{out}}$ and $f_{\vec{v}}^{\text{in}}$ of the k order nodes \vec{v} are preserved.

Algorithm 1 ComputeHYPA(S, k): Compute k th order HYPAscores for sequence dataset S.

Input: S (sequences), k (desired order)

Output: HYPAscore for all k -th order paths

1: $G^k \leftarrow \text{DeBruijnGraph}(S, k)$ # Construct k th order graph

2: $\Xi \leftarrow \text{fitXi}(G^k, \text{tolerance})$ # Optimization (Algorithm 2 in Appendix A.1)

3: **for** $(\vec{v}, \vec{w}) \in G^k$ **do**

4: HYPAscore $^{(k)}(\vec{v}, \vec{w}) \leftarrow \text{Pr}(x_{vw} \leq (\vec{v}, \vec{w}) \mid m, \Xi)$

 # Compute CDF

5: **return** HYPAscore $^{(k)}$

HYPAs Algorithm. The random De Bruijn graph model of order k introduced above is the basis for the HYPAs algorithm to detect path anomalies (see Algorithm 1). In particular, we have argued that the distribution of edge weights in the statistical ensemble of random realizations are jointly described by a multivariate hypergeometric distribution. We can now use the marginals of this distribution to calculate the distribution of edge weights for each edge individually as:

$$\Pr(X_{\vec{v}\vec{w}} = f(\vec{v}, \vec{w})) = \binom{\sum_{ij} \Xi_{ij}}{m}^{-1} \binom{\Xi_{vw}}{f(\vec{v}, \vec{w})} \binom{\sum_{ij} \Xi_{ij} - \Xi_{vw}}{m - f(\vec{v}, \vec{w})}, \quad (1)$$

where $m = \sum_v f_v^{\text{out}} = \sum_v f_v^{\text{in}}$ is the sum of all weights in the graph and $X_{\vec{v}\vec{w}}$ is a random variable assuming the weight of edge (\vec{v}, \vec{w}) in a random realization of a k -th order De Bruijn graph. We use these marginal distributions to define the HYPAs $^{(k)}$ score for a path $\vec{v}\vec{w}$ of length k with observed frequency $f(\vec{v}, \vec{w})$ as the cumulative distribution corresponding to Eq. (1):

$$\text{HYPAs}^{(k)}(\vec{v}, \vec{w}) := \Pr(X_{\vec{v}\vec{w}} \leq f(\vec{v}, \vec{w})) \quad (2)$$

Since the HYPAs $^{(k)}$ score is a probability, it assumes values in $[0, 1]$. Paths whose HYPAs $^{(k)}$ scores are close to zero are likely to be under-represented compared to the random baseline. That is, the probability to obtain at random a frequency for this path that is lower or equal to the frequency in the data is small. On the other hand, a path whose HYPAs $^{(k)}$ score is close to one is likely to be over-represented. That is, the frequency obtained at random for a given path is likely

to be smaller than the one observed in the data. A path that has a $\text{HYPA}^{(k)}$ score of 0.5 is equally likely to observe higher or lower frequency at random, and thus shows the least indication of an anomaly. Users of our method can set a discrimination threshold $\alpha \in (0, 1]$, at which they can classify as under-represented any path (\vec{v}, \vec{w}) with $\text{HYPA}^{(k)}(\vec{v}, \vec{w}) < \alpha$ and as over-represented any path (\vec{v}, \vec{w}) with $\text{HYPA}^{(k)}(\vec{v}, \vec{w}) > 1 - \alpha$.

Computational Complexity. To detect anomalous paths of length k in a graph G we need to compute a HYPA score for each weighted edge in a k -th order De Bruijn graph as defined in Def. 2.1. To construct the weights of those edges we must count all subpaths of length k in S , which requires a single pass through the $N := \sum_{i=1}^n l_i$ “node traversals” on the n paths contained in S . This implies that the asymptotic runtime of HYPA is in $O(N + \Delta^k(G))$, where $\Delta^k(G)$ is the number of edges in a k -th order De Bruijn graph model G^k of paths in G . The following lemma gives an upper bound for $\Delta^k(G)$:

LEMMA 1. *Let $G = (V, E)$ be a directed graph and let $k \in \mathbb{N}$ be the order of a De Bruijn graph model of paths in G . $\Delta^k(G)$ is bounded above by $|V|^2 \lambda_1^k$, where λ_1 is the leading eigenvalue of the binary adjacency matrix of G .*

Due to space constraints, we prove this lemma in Appendix A.2. Using Lemma 1, we find that the computational complexity of HYPA is in $O(N + |V|^2 \lambda_1^k)$, where N is the size of the data S , $|V|$ is the number of nodes in G , k is the order of the De Bruijn graph model, and λ_1 is the leading eigenvalue in the spectrum of G . This shows that the runtime of our method linearly depends on the size N of the data, with an additional additive term depending on the topology of graph G and the order k . The algebraic connectivity λ_1 of graph G captures how the size of k -th order De Bruijn graph models grows with the order k . This implies that – for sparse real-world graphs, moderate values of k and above a sufficiently large value of N – our method scales linearly with the size of the data.

4 EXPERIMENTS

Table 1: Description of empirical data sets, with λ_1 denoting the largest eigenvalue of the adjacency matrix of graph G , $N = \sum_i l_i$ being the sum of all path lengths, l^{\max} and $\langle l \rangle$ denoting maximum and average path length.

Data	Graph $G = (V, E)$			Sequences S				N
	$ V $	$ E $	λ_1	Total	Unique	l^{\max}	$\langle l \rangle$	
Journals	283	1743	26.19	480496	309565	35	14.8	$1.64 \cdot 10^8$
Tube	268	646	3.99	4295731	67015	35	6.75	$2.89 \cdot 10^7$
Flights	382	6933	56.55	185871	88539	10	2.48	$4.61 \cdot 10^5$
Wiki	100	1598	21.47	29682	7431	21	1.64	$4.88 \cdot 10^4$
Hospital	75	1138	37.01	28422	2561	5	1.19	$3.37 \cdot 10^4$

We now show that we can use the scores calculated by HYPA to detect paths with anomalous frequencies. We first validate our method in both synthetically generated data with known implanted anomalies and in real data with ground truth path anomaly labels generated by numerical simulation. Then, we apply our method to empirical time series data on transportation, information, and social networks, showing that the under- and over-represented

paths fall into different classes that can be validated using semantic and geographic features.

4.1 Baseline Method

In the below experiments, we compare HYPA to a simple frequency-based anomaly detection (FBAD) of our own design. We note that despite similar problem settings, the methods for hypothesis testing on human trails presented in [8, 44] are not directly comparable with our work because the output is Bayesian evidence for a hypothesis on an entire dataset (a single number), whereas we are interested in edge-level analysis. However, in future work we could use HYPA to generate hypotheses to be tested using these methods. Further, we did not compare with a method like [39] because, while based on detecting significant deviations from a Markov chain model, this method assumes that the data is given as one long sequence and detects anomalous subsequences, which does not correspond to any of the datasets we analyze here.

We now briefly describe FBAD and provide more details including pseudocode in Algorithm 5 of Appendix A.5. FBAD computes the average μ and standard deviation σ of path counts and employs a user-defined threshold α to detect over- and under-represented paths. In particular, a path is labeled as over-represented if its frequency exceeds $\mu + \sigma\alpha$, and as under-represented if its frequency is smaller than $\mu - \sigma\alpha$.

4.2 Synthetic Data

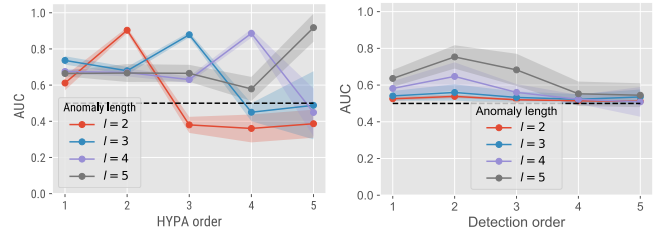


Figure 3: $\text{HYPA}^{(k)}$ detects injected path anomalies at the correct length with high accuracy. Each curve corresponds to one length l of generated anomalous paths, and represents the performance of classifying the anomalous paths using HYPA (left) or the naive FBAD method (right) applied at increasing orders k . HYPA detects the exact generated anomalies, i.e., performs highly at $k = l$. FBAD only performs relatively well in detecting short sub-paths (e.g., $k = 2$) of longer anomalies (e.g., $l = 5$). Averages and standard errors are over 10 independent experiments.

To validate our method, we use a stochastic model generating synthetic sets of paths with varying lengths, in which a known set of paths with given length l exhibit anomalous frequencies. Adopting the well-known Erdős-Rényi model [21], our model generates paths in a random directed graph G with n nodes, where pairs of nodes are connected with probability p . Following Definition 3.2, the random model generates paths based on an edge-weighted random walk in a k -th order De Bruijn graph of paths in the random graph G . By selectively changing transition probabilities in T^l (cf.

Definition 3.2), we introduce anomalous frequencies for a known set of paths at length l . Since all paths longer than l are generated by a (Markovian) random walk on a De Bruijn graph with order l , these paths will not exhibit anomalous frequencies beyond those expected from the anomalous frequencies of paths of length l . For details of the random path construction, see the pseudocode in Algorithms 3 and 4 in Appendix A.3. In the following we report results for graphs G with $n = 50$ nodes and an edge probability of $p = 0.05$ (conclusions do not depend on those parameters).

We test whether HYP A detects anomalous path frequencies (i) with high accuracy, and (ii) at the correct length l introduced by our model. To this end, we calculate the performance of HYP A in a binary classification experiment, categorizing path frequencies as anomalous based on variable discrimination thresholds α for the $\text{HYP A}^{(k)}$ scores at different orders k . For each threshold α , we compute the true and false positive rates of detected anomalies w.r.t. the known ground truth and obtain a receiver operating characteristic (ROC) curve, for which we can calculate the area under the curve (AUC). For each length $l \in [2, 5]$ of generated anomalous paths and each order $k \in [1, 5]$, we repeat this experiment 10 times. Each curve in Fig. 3 presents the mean and the standard error of the AUC for anomalies detected at varying orders k , for a given anomaly length l . For $k \neq l$, we use as ground-truth the paths of length k that either include or are included in an anomalous path of length l generated by the synthetic model. For each l we observe that HYP A with the ‘‘correct’’ order $k = l$ is able to identify ground truth anomalies with high accuracy ($\text{AUC} \approx 0.9$, left plot), while the baseline FBAD method is unable to detect path anomalies with high accuracy at any order, regardless of the order used for detection (max $\text{AUC} \approx 0.78$, right plot).

4.3 Empirical Data

We now apply our method to five empirical datasets capturing paths in transportation systems, information networks, and dynamic social networks: *Tube* comprises sequences of stations traveled in the London Underground [22]; *Flights* comprise 5% of all travel itineraries of passengers flying in the US in the first quarter of 2018 [48]; *Journals* represent citations between a subset of High-Energy Physics journals [26]; *Hospital* contains face-to-face contact sequences of people occupying four roles (patients, nurses, doctors, administrators) in a hospital ward [49]; and *Wiki* contains click-stream data from the ‘‘Wikipedia’’ game where players had to find a specified target page starting from a given Wikipedia page by following hyperlinks. Basic characteristics of these datasets are presented in Table 1 (see Appendix A.6 for details on filtering and processing of the data).

Detection of ground truth anomalies. As exemplified in Fig. 2(c) and implied by Definition 3.1, path anomalies can, in principle, also be discovered through large-scale numerical simulations. To achieve this for order k we can randomize the data by replacing every observed path with a $(k - 1)$ -order random walk of the same length starting in the same node. A large number of such simulations generates empirical frequency distributions of all paths with given length k . We can then use those distributions to infer which paths in the empirical data are over- or under-represented. A detailed description of this approach can be found in Appendix A.7. While

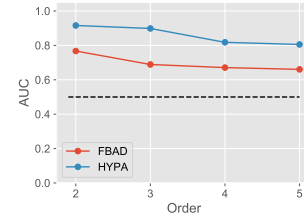


Figure 4: HYP A outperforms FBAD in detecting anomalous paths in the London Tube data. For this data set, ground truth anomalies can be established using computationally expensive numerical simulations. We apply both methods at various orders k and measure their performance in predicting the ground truth. At all detection orders k , HYP A considerably outperforms FBAD, illustrating the inadequacy of frequency-based methods for path anomalies.

it is prohibitively expensive for large data sets, it enables us to generate a proxy for *ground truth path anomalies* in the London Tube data. In this case, each randomized version of the data is generated by performing more than 4.8 million random walks with an average length of 14.8 steps in the (weighted) graph topology. We repeat this multiple times to obtain ground truth labels for over- and under-represented paths (details in Appendix A.7). Repeating the experiment from Section 4.2, these ground truth labels allow us to compare the performance of HYP A against the baseline frequency-based detection (FBAD). We use the London Tube data set for our experiment because its topology is sufficiently small and sparse to allow for this expensive numerical approach. The results in Fig. 4 show that (i) HYP A is able to detect ground truth path anomalies with high accuracy, (ii) our analytical approach outperforms the detection performance of the baseline frequency-based detection (FBAD) at all orders k , and (iii) we obtain an increase in prediction performance of approximately 30% at order $k = 3$.

Path motifs. In Fig. 5 we study how anomalous paths detected by HYP A at $k = 2$ are distributed in the three data sets *Wiki*, *Journals*, and *Hospital*. We focus on five distinct motifs (horizontal axis in plots) where, e.g. \overrightarrow{ABC} represents paths traversing distinct nodes and \overrightarrow{ABA} represents paths that start and end in the same node but pass through another node. While Fig. 5 highlights the absence of a universal pattern of motif anomalies across systems, some of the observed differences can be intuitively attributed to system-specific mechanisms. For instance, paths of the type \overrightarrow{ABA} are among the most over-represented paths in *Wiki*, which is likely a result of users using the ‘back’ button of their browser while playing the game. In *Journals*, citation paths of the type \overrightarrow{ABC} through three distinct journals are both most over-represented and least under-represented. This indicates (i) a hierarchy in journals in terms of knowledge flows through citations (papers in A implicitly rely on papers in C) and (ii) that knowledge flow is preferentially routed through certain sets of (probably multi-disciplinary) journals B .

Tube Geographic Hypothesis. We next use HYP A to test a hypothesis about the geographic embedding and over- and under-represented paths in *Tube*. Intuitively, we expect people to use

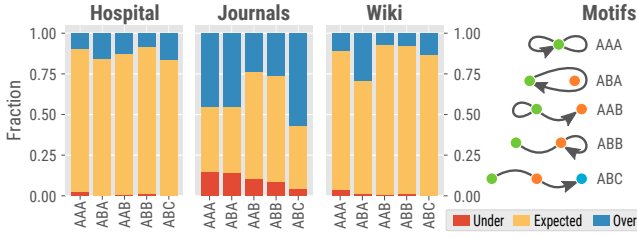


Figure 5: The distribution of over and under represented paths ($k = 2$) across motifs, i.e., recurrent types of paths, is system dependent. For instance, in click stream data the motif *ABA* is over-represented much more than the others due to the user hitting the ‘back’ button in the browser. The discrimination threshold used for detection was $\alpha = 0.01$.

public transportation like the London Underground preferentially for longer distance trips, such as commutes to and from work, while avoiding trips with very short, walk-able distances. This leads to the hypothesis that over-represented itineraries span larger geographic distances compared to those that are under-represented.

We use HYPA to test this hypothesis. We first compute $\text{HYPA}^{(k)}$ scores for values $k = 1, \dots, 6$. We then detect over- and under-represented paths based on discrimination threshold $\alpha = 0.001$. We can use the detected anomalies to generate a decomposition of a k -th order De Bruijn graph model of paths based on under- and over-represented edge weights. The resulting decomposition for $k=2$ are shown in Fig. 6 (left column), where the nodes are placed according to geographic positions of London Tube stations. The network of under-represented paths (top) exhibits high clustering and an absence of long chains, highlighting that it is predominantly paths spanning short geographic distances that are under-represented. In contrast, the network of over-represented paths (bottom) shows long chains, which supports the hypothesis that paths spanning longer distances are occurring more often than expected at random.

To substantiate this intuition, in Fig. 6 we show how geographic distances between start and end stations in over- and under-represented itineraries at $k = 2$ are distributed. The distance distribution of under-represented itineraries is shifted towards smaller distances, while the over-represented distribution is shifted towards larger distances, which supports our hypothesis. We find that the shift in distance distribution at order two is significant, witnessed by a p -value ≈ 0 of a Mann-Whitney U-test (Table 2). Because the null model allows for paths starting and ending at the same node, there is a peak in the distribution of under-represented paths (see Fig. 6) at distance zero. This is due to such paths being absent in the data.

At $k > 2$ paths starting and ending at the same node are not present, hence repeating the test provides a better support for the geographic hypothesis. As shown in Table 2, indeed the over-represented trips are longer on average.

Efficiency and Balance in Flight Itineraries. We now show how HYPA can be used to test hypotheses about specific types of paths. We demonstrate this in a large data set containing flight itineraries of airline passengers in the United States. Our first hypothesis is that return flights (*ABA*) are significantly over-represented, since

Table 2: The median distance in kilometers between origins and destinations is significantly larger for over-represented paths of length k compared to under-represented paths in the London Tube, as shown by the p -value one-sided Mann-Whitney U-test. The discrimination threshold on HYPA (2) scores was $\alpha = 0.001$.

$\text{HYPA}^{(k)}$	$k = 2$	$k = 3$	$k = 4$	$k = 5$	$k = 6$
Under [km]	0.00	2.38	3.29	4.60	5.43
Over [km]	2.20	2.93	3.79	5.21	5.63
p -value	$< 10^{-170}$	$< 10^{-7}$	$< 10^{-4}$	0.006	0.08

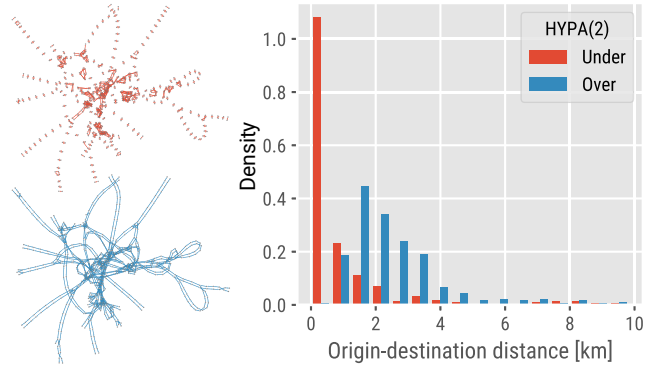


Figure 6: For any order k and discrimination threshold α , HYPA acts as a filter on the k th order De Bruijn graph, separating over-represented (blue) and under-represented (red) paths of length k . In the Tube data, Under-represented paths detected by HYPA are tightly clustered, corresponding to avoidance of geographically short trips. Over-represented paths are arranged in chains, corresponding to longer distance trips (as in daily suburban commutes). On the right, we show a histogram of geographic distances, to illustrate that both over- and under-represented paths detected by HYPA correlate with the geography of the system.

passengers often leave from and return to the same airport. We first compute HYPA scores for $k = 2$. We then separate return from non-return flights and compute the fraction of over-represented paths in each for varying discrimination thresholds α . The results in Table 3 support the hypothesis that return flights are strongly over-represented with respect to the random baseline.

Table 3: Fractions of over-represented paths ($k = 2$) between airports for return flights (5840 unique paths) and non-return flights (409254 unique paths) at different discrimination thresholds α .

α	0.05	0.01	0.001	0.0001	0.00001
Return	0.915	0.851	0.760	0.688	0.628
Non-return	0.340	0.130	0.023	0.004	0.001

However, we still observe a number of over-represented non-return flight paths. We hypothesize that many over-represented paths connect small airports to large airports via regional hubs. This means that a relatively short distance trip (e.g. from ORL to ATL) is

required before a flight from the regional hub to a relatively distant destination (e.g. ATL to LAX). Rather than classifying airports by their size and role in the network, we test this hypothesis by defining *distance balance*, a measure that captures to what extent one leg of a trip dominates the total trip distance. In a perfectly balanced trip (ABC), the distance of the two legs is equal, e.g. $d(A, B) = d(B, C)$. The most common example of a perfectly balanced trip is the return trip, where $A = C$. In an imbalanced trip, one of the legs of the trip is much larger. We define balance by the ratio $\frac{d(A, B) - d(B, C)}{d(A, B) + d(B, C)}$. It approaches -1 or 1 when the distance of one leg of the trip is much greater than on the other. We expect flights with extreme values to be over-represented as they represent long distance flights that start from small, local airports, fly a short distance to a regional hub, then on to a much further off destination (as well as the reverse). The distribution of balance for over- and under-represented paths of length two ($\alpha = 0.05$) is shown in Fig. 7 (top right). We find very few under-represented flights near extreme values of balance, while a larger fraction of over-represented paths are found near -1 and 1. This supports our hypothesis that unbalanced flights tend to be more over-represented than balanced flights.

We conclude this analysis by formulating hypotheses based on a notion of *efficiency* for airline trips. We measure efficiency as the ratio of the distance between source and destination, $d(A, C)$, with the actual flight distance, $d(A, B) + d(B, C)$. Using this measure, a straight line between airports A, B and C would have a maximum efficiency of 1, while a low efficiency trip implies that the actual flight distance is much larger than the straight line distance between the origin and destination. We hypothesize that highly efficient paths are over-represented, while inefficient paths are under-represented in the data. The bottom left plot of Fig. 7 shows a large peak in the fraction of under-represented paths at very low efficiency, then a steady decrease in under-represented paths as efficiency increases. In the bottom right figure we see that after return flights are accounted for (peak at efficiency 0), the fraction of over-represented paths increases monotonically with efficiency. These results indicate that more efficient paths are indeed more likely to be over-represented, and that the more efficient a path is, the less likely it is to be under-represented.

4.4 Scalability

We finally validate the theoretical analysis of computational complexity in section 4.4 through an experimental evaluation of scalability in empirical data. We measure the time needed to detect path anomalies for (i) varying orders k in a data set of fixed size N and (ii) a fixed order k and data with varying size N . Fig. 8 reports the time needed to run HYPAs on a single core of an Intel i7-7600U CPU. All values are averages of ten measurements. The left panel in Fig. 8 confirms that the runtime of our algorithm scales as an exponent of k , where the basis of the exponent depends on the algebraic connectivity of the graph. We note however that, even for a data set with more than four million paths the detection of anomalies up to length eight takes less than two minutes. The right panel in Fig. 8 confirms that our analytical approach is suitable for large data sets. In particular, the experimental results are aligned with our theoretical analysis of computational complexity in Section 3.2, which predicts that below a critical sum of path lengths

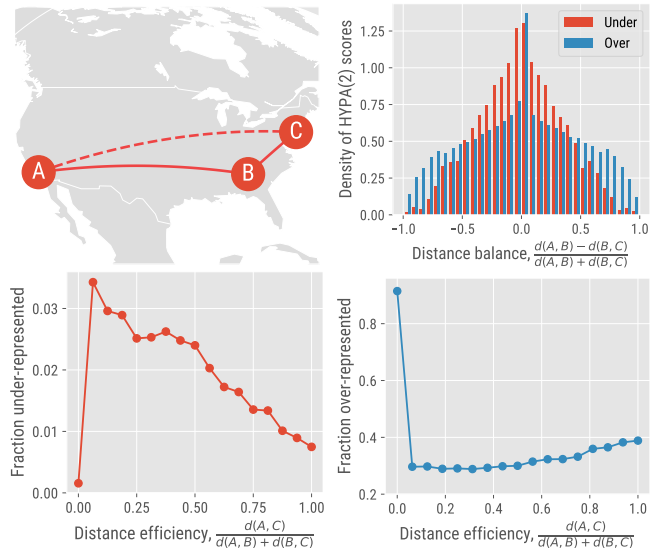


Figure 7: Top-right: extreme values of *balance* correspond to over-represented paths, confirming that short flights followed by long flights are typical (e.g. flights to a regional hub, then a national hub). Bottom-left: The fraction of over- and under-represented paths in data on flight itineraries varies with the efficiency of the itinerary, which we define as the ratio of the straight line distance $d(A, C)$ between the origin and the destination and the total flight distance $d(A, B) + d(B, C)$. After return flights are accounted for, the fraction of under-represented paths decreases with efficiency, and vice versa for over-represented paths.

N , the runtime of HYPAs is dominated by the number of paths of length k . This explains why for small values of N we observe an exponential increase of runtime as the size of the k -dimensional De Bruijn graph model approaches the theoretical upper limit of $|V|^2 \lambda_1^k$. For large values of N , the runtime of HYPAs is dominated by a linear term that is due to the single pass through the data, while the calculation of HYPAs scores is independent of the size of the data. This confirms that the analytical approach underlying our algorithm makes it suitable to analyse big time series data on networks.

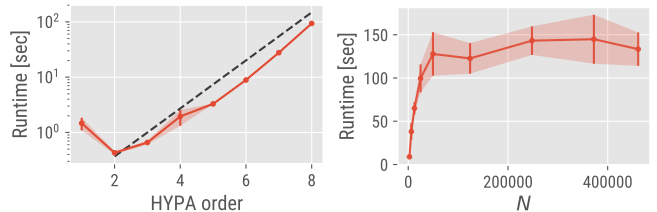


Figure 8: Empirical scalability of HYPAs. Left: Required time to detect path anomalies of length k for the Tube data. Right: Runtime in Flights data for detection order $k = 1$ and varying data size N randomly sampled from the data. All data points correspond to the mean of ten repeated measurements, with the standard deviations shown as bars.

5 CONCLUSION

We have presented a novel approach for the unsupervised detection of path anomalies in time series data on networks. Providing a new theoretical basis for anomaly detection in graphs, our work advances the state-of-the-art in multiple directions. We first introduce the problem of path anomaly detection and show that it cannot be addressed by existing frequency-based anomaly detection techniques. Projecting paths in a (first-order) graph onto higher-order De Bruijn graphs, we show that path anomaly detection can be reduced to the detection of anomalous edge weights in a higher-order graph space. Building on an analytically tractable null model of higher-order De Bruijn graphs, we obtain a parameter-free and scalable method that allows us to assess statistical deviations in the frequencies of paths traversing the nodes of a graph.

Compared to works focused on finding optimal higher-order models of time series data, our approach allows to detect which individual paths exhibit significant deviations from a random baseline. Our method opens new perspectives for model order reduction in higher-order network models, which can help to alleviate some of the scalability issues. To facilitate the reproducibility of our findings and applications of our method in real scenarios, a python implementation of our framework will be made available online [7].

ACKNOWLEDGEMENTS

Ingo Scholtes acknowledges support by the Swiss National Science Foundation, grant 176938. LaRock and Eliassi-Rad were supported in part by NSF IIS-1741197, the Army Research Laboratory Cooperative Agreement W911NF-13-2-0045, and the Under Secretary of Defense for Research and Engineering under Air Force Contract No. FA8702-15-D-0001. Any views, opinions, findings, conclusions or recommendations expressed in this material are solely those of the authors.

REFERENCES

- [1] R. Agrawal and R. Srikant. Mining sequential patterns. In *ICDE*, pages 3–14, 1995.
- [2] L. Akoglu and C. Faloutsos. Event detection in time series of mobile communication graphs. In *Army Science Conference*, pages 77–79, 2010.
- [3] L. Akoglu, H. Tong, and D. Koutra. Graph based anomaly detection and description: a survey. volume 29, pages 626–688, 2015.
- [4] M. Atzmueller. Detecting community patterns capturing exceptional link trails. In *ASONAM*, pages 757–764, 2016.
- [5] M. Atzmueller, A. Schmidt, and D. Arnu. Sequential modeling and structural anomaly analytics in industrial production environments. In *LWDA*, pages 283–290, 2016.
- [6] M. Atzmueller, A. Schmidt, and M. Kibanov. Dashtrails: an approach for modeling and analysis of distribution-adapted sequential hypotheses and trails. In *WWW*, pages 553–558, 2016.
- [7] B. authors. hypa software package. to be published at github.com, 2019.
- [8] M. Becker, F. Lemmerich, P. Singer, M. Strohmaier, and A. Hotho. Mixedtrails: Bayesian hypothesis comparison on heterogeneous sequential data. *Data Mining and Knowledge Discovery*, 31(5):1359–1390, 2017.
- [9] R. Bertens, J. Vreeken, and A. Siebes. Keeping it short and simple: Summarising complex event sequences with multivariate patterns. In *KDD*, 2016.
- [10] C. C. Bilgin and B. Yener. Dynamic network evolution: Models, clustering, anomaly detection. *IEEE Networks*, 2006.
- [11] B. Boden, S. Gunnemann, and T. Seidl. Tracing clusters in evolving graphs with node attributes. In *CIKM*, pages 2331–2334, 2012.
- [12] I. Cadez, D. Heckerman, C. Meek, P. Smyth, and S. White. Visualization of navigation patterns on a web site using model-based clustering. In *KDD*, pages 280–284, 2000.
- [13] G. Casiraghi and V. Nanumyan. Generalised hypergeometric ensembles of random graphs: The configuration model as an urn problem. *arXiv:1810.06495 [physics]*, 2018.

- [14] G. Casiraghi, V. Nanumyan, I. Scholtes, and F. Schweitzer. From relational data to graphs: Inferring significant links using generalized hypergeometric ensembles. In *Social Informatics*, pages 111–120, 2017.
- [15] S. Chakrabarti, S. Sarawagi, and B. Dom. Mining surprising patterns using temporal description length. In *VLDB*, volume 98, pages 606–617, 1998.
- [16] V. Chandola, A. Banerjee, and V. Kumar. Anomaly detection: A survey. *ACM computing surveys*, 41(3):15, 2009.
- [17] V. Chandola, A. Banerjee, and V. Kumar. Anomaly detection for discrete sequences: A survey. *IEEE TKDE*, 24(5):823–839, 2012.
- [18] V. Chandola, V. Mithal, and V. Kumar. Comparative evaluation of anomaly detection techniques for sequence data. In *ICDM*, pages 743–748, 2008.
- [19] N. G. de Bruijn. A combinatorial problem. *Koninklijke Nederlandse Akademie v. Wetenschappen*, 49:758–764, 1946.
- [20] M. El-Sayed, C. Ruiz, and E. A. Rundensteiner. Fs-miner: efficient and incremental mining of frequent sequence patterns in web logs. In *WIDM*, 2004.
- [21] P. Erdos and A. Rényi. On the evolution of random graphs. *Publ. Math. Inst. Hung. Acad. Sci.*, 5(1):17–60, 1960.
- [22] T. for London. Rolling origin and destination survey (rods)database. <http://www.tfl.gov.uk/info-for/open-data-users/our-feeds>, 2014.
- [23] E. N. Gilbert. Random graphs. *The Annals of Mathematical Statistics*, 30(4):1141–1144, 1959.
- [24] M. Gupta, J. Gao, C. C. Aggarwal, and J. Han. Outlier detection for temporal data: A survey. *IEEE TKDE*, 26(9):2250–2267, 2014.
- [25] R. Gwadera, M. Atallah, and W. Szpankowski. Markov models for identification of significant episodes. In *SDM*, pages 404–414, 2005.
- [26] INSPIRE. Inspire hep. <http://inspirehep.net/info/hep/api>, 2018.
- [27] E. Keogh, S. Lonardi, C. A. Ratanamahatana, L. Wei, S.-H. Lee, and J. Handley. Compression-based data mining of sequential data. *Data Mining and Knowledge Discovery*, 14(1):99–129, 2007.
- [28] R. Lambiotte, M. Rosvall, and I. Scholtes. From networks to optimal higher-order models of complex systems. *Nature Physics*, 15:313–320, April 2019.
- [29] T. Lane and C. E. Brodley. An empirical study of two approaches to sequence learning for anomaly detection. *MLJ*, 51(1):73–107, 2003.
- [30] R. Laxhammar and G. Falkman. Online learning and sequential anomaly detection in trajectories. *TPAMI*, 36(6):1158–1173, 2014.
- [31] F. Lemmerich, M. Becker, P. Singer, D. Helic, A. Hotho, and M. Strohmaier. Mining subgroups with exceptional transition behavior. In *KDD*, pages 965–974, 2016.
- [32] I. Melnyk, B. Matthews, H. Valizadegan, A. Banerjee, and N. Oza. Vector autoregressive model-based anomaly detection in aviation systems. *J. of Aerospace Information Systems*, pages 161–173, 2016.
- [33] J. K. Merikoski. On the trace and the sum of elements of a matrix. *Linear Algebra and its Applications*, 60:177 – 185, 1984.
- [34] M. Molloy and B. Reed. A critical point for random graphs with a given degree sequence. *Random Structures & Algorithms*, 6(2-3):161–180, 1995.
- [35] C. C. Noble and D. J. Cook. Graph-based anomaly detection. In *KDD '03*, 2003.
- [36] G. Palla, N. Páll, A. Horváth, K. Molnár, B. Tóth, T. Kováts, G. Surján, T. Vicsek, and P. Pollner. Complex clinical pathways of an autoimmune disease. *J. of Complex Networks*, 6(2):206–214, 2017.
- [37] T. P. Peixoto and M. Rosvall. Modelling sequences and temporal networks with dynamic community structures. *Nature communications*, 8(1):582, 2017.
- [38] M. Rosvall, A. V. Esquivel, A. Lancichinetti, J. D. West, and R. Lambiotte. Memory in network flows and its effects on spreading dynamics and community detection. *Nature communications*, 5, 2014.
- [39] R. Sadodddin, J. Sander, and D. Rafiei. Finding Surprisingly Frequent Patterns of Variable Lengths in Sequence Data. In *Proceedings of the 2016 SIAM International Conference on Data Mining*, pages 27–35. Society for Industrial and Applied Mathematics, June 2016.
- [40] V. Salnikov, M. T. Schaub, and R. Lambiotte. Using higher-order Markov models to reveal flow-based communities in networks. *Sci. Rep.*, 6:23194, 2016.
- [41] I. Scholtes. When is a network a network?: Multi-order graphical model selection in pathways and temporal networks. In *KDD*, pages 1037–1046, 2017.
- [42] I. Scholtes, N. Wider, R. Pfitzner, A. Garas, C. J. Tessone, and F. Schweitzer. Causality-driven slow-down and speed-up of diffusion in non-markovian temporal networks. *Nature Communications*, 5:5024, 2014.
- [43] S. Servan-Schreiber, M. Riionato, and E. Zraggen. Prosecco: Progressive sequence mining with convergence guarantees. In *ICDM*, pages 417–426, 2018.
- [44] P. Singer, D. Helic, A. Hotho, and M. Strohmaier. Hyptrails: A bayesian approach for comparing hypotheses about human trails on the web. In *WWW*, pages 1003–1013, 2015.
- [45] P. Smyth. Clustering sequences with hidden markov models. In *NIPS*, pages 648–654, 1997.
- [46] A. Tajer, V. V. Veeravalli, and H. V. Poor. Outlying sequence detection in large data sets: A data-driven approach. *IEEE Signal Processing Magazine*, 31(5):44–56, 2014.
- [47] E. Tonnelier, N. Baskiotis, V. Guigue, and P. Gallinari. Anomaly detection in smart card logs and distant evaluation with twitter: a robust framework. *Neuro-computing*, 298:109–121, 2018.

- [48] R. TransStat. Origin and destination survey database. http://www.transtats.bts.gov/Tables.asp?DB_ID=125, 2018.
- [49] P. Vanhems, A. Barrat, C. Cattuto, J. Pinton, and N. Khanafer. Estimating potential infection transmission routes in hospital wards using wearable proximity sensors. *PLoS ONE*, 8(9):e73970, 09 2013.
- [50] S. Walk, P. Singer, and M. Strohmaier. Sequential action patterns in collaborative ontology-engineering projects: A case-study in the biomedical domain. In *CIKM*, pages 1349–1358, 2014.
- [51] R. West and J. Leskovec. Human wayfinding in information networks. In *WWW*, pages 619–628, 2012.
- [52] J. Xu, T. L. Wickramaratne, and N. V. Chawla. Representing higher-order dependencies in networks. *Science Advances*, 2(5), 2016.
- [53] D. Zhou, J. He, Y. Cao, and J.-s. Seo. Bi-level rare temporal pattern detection. In *ICDM*, pages 719–728, 2016.

A SUPPLEMENTARY MATERIAL

To facilitate reproducibility, we use this supplement for the following: (i) describe in detail the algorithm we use to redistribute values in the Ξ matrix (Section 3); (ii) provide a proof for Lemma 1, which was omitted from the main text due to space constraints; (iii) provide details and pseudocode for the synthetic model used for the experiment in Fig. 3; (iv) explain in detail how the results in Fig. 3 were generated; (v) provide pseudocode for the naive baseline method FBAD; (vi) provide details of the construction and preprocessing of the real world datasets (Section 4); and finally (vii) describe in more detail the procedure we used to generate ground truth path anomalies.

A.1 Ξ Redistribution

In Section 3.2 we briefly describe a simple algorithm to redistribute the values in the matrix Ξ such that it respects the constraints imposed by the k -order De Bruijn graph while also preserving the weighted in- and out-frequencies of the k -order nodes when used for sampling. Algorithm 2 shows the exact procedure we employ.

Algorithm 2 fitXi(G^k , tolerance): *Adjust entries of Ξ to match expected frequencies (based on Ξ) to observed frequencies (based on W) within “tolerance” error.*

Input: G^k (k -order De Bruijn graph), tolerance
Output: Ξ

- 1: $f_v^{\text{out}} \leftarrow \sum_x f(v, x)$ # weighted out-degrees
- 2: $f_v^{\text{in}} \leftarrow \sum_x f(x, v)$ # weighted in-degrees
- 3: $m \leftarrow \sum_v f_v^{\text{out}}$ # sum of all weights
- 4: $\Xi_{vw} \leftarrow f_v^{\text{out}} \cdot f_w^{\text{in}}$ # initialize matrix for all $v, w \in G^k$
- 5: $M \leftarrow \sum_{vw} \Xi_{vw}$
- 6: **if** edge (v, w) not possible in G^k **then**
- 7: $\Xi_{vw} \leftarrow 0$ # ensure edge (v, w) cannot be sampled
- 8: **repeat**
- 9: $\hat{f}_v^{\text{in}} \leftarrow \frac{\sum_x \Xi_{xv}}{m} \cdot \frac{M}{\sum_{vw} \Xi_{vw}}$ # Expectation for in-degrees
- 10: $\Xi_{vw} \leftarrow \Xi_{vw} \cdot \frac{f_w^{\text{in}}}{\hat{f}_v^{\text{in}}}$ # Correction for in-degrees
- 11: $\hat{f}_v^{\text{out}} \leftarrow \frac{\sum_x \Xi_{vx}}{m} \cdot \frac{M}{\sum_{vw} \Xi_{vw}}$ # Expectation for out-degrees
- 12: $\Xi_{vw} \leftarrow \Xi_{vw} \cdot \frac{f_v^{\text{out}}}{\hat{f}_v^{\text{out}}}$ # Correction for out-degrees
- 13: **until** $\text{RMSE}(f_v^{\text{out}}, \hat{f}_v^{\text{out}}) + \text{RMSE}(f_v^{\text{in}}, \hat{f}_v^{\text{in}}) \leq \text{tolerance}$
- 14: **return** Ξ

A.2 Proof of Computational Complexity

LEMMA 1. *Let $G = (V, E)$ be a directed graph and let $k \in \mathbb{N}$ be the order of a De Bruijn graph model of paths in G . $\Delta^k(G)$ is bounded above by $|V|^2 \lambda_1^k$, where λ_1 is the leading eigenvalue of the binary adjacency matrix of G .*

PROOF. We first note that for a fully connected graph G with $|V|$ nodes and $E = V^2$ we trivially have $\Delta^k(G) = |V|^{k+1}$. This follows from the fact that every possible sequence of $k + 1$ nodes is a path of length k in a full graph, i.e. a k -th order De Bruijn graph model has $|V|^{k+1}$ edges.

Let us now consider a graph G with arbitrary topology and let A be the binary adjacency matrix of G , where one-elements indicate

the presence and zero-elements indicate the absence of an edge. We can compute the number of distinct paths of length k in G as $\sum_i \sum_j (\mathbf{A}^k)_{ij}$, where \mathbf{A}^k is the k -th power of adjacency matrix \mathbf{A} . This directly follows from the definition of matrix multiplication, leading to the fact that each element $(\mathbf{A}^k)_{ij}$ in the k -th power of \mathbf{A} counts distinct paths of length k between nodes i and j .

To prove the lemma, we use the following two facts. First, the sum of all elements in any matrix \mathbf{B} is equal to $\text{tr}(\mathbf{J}\mathbf{B})$, i.e., the sum of *diagonal* elements in the matrix product $\mathbf{J}\mathbf{B}$, where \mathbf{J} is the $|V| \times |V|$ all-ones matrix. Second, if \mathbf{B}, \mathbf{C} are positive semi-definite matrices, from the Cauchy-Schwartz inequality follows $\text{tr}(\mathbf{C}\mathbf{B}) \leq \text{tr}(\mathbf{C})\text{tr}(\mathbf{B})$ [33]. We can thus write:

$$\Delta^k(G) = \sum_{i=1}^{|V|} \sum_{j=1}^{|V|} (\mathbf{A}^k)_{ij} = \text{tr}(\mathbf{J}\mathbf{A}^k) \leq \text{tr}(\mathbf{J}) \cdot \text{tr}(\mathbf{A}^k)$$

We now recall (i) that the trace of any square matrix is equal to the sum of its eigenvalues, (ii) that the eigenvalue sequence of an $|V| \times |V|$ all-one matrix \mathbf{J} is $|V|, 0, \dots, 0$, and (iii) that the eigenvalues of the k -th power \mathbf{A}^k of a matrix are the k -th powers of eigenvalues of \mathbf{A} . We can thus write:

$$\Delta^k(G) \leq \text{tr}(\mathbf{J}) \cdot \text{tr}(\mathbf{A}^k) = |V| \cdot \sum_{i=1}^{|V|} \lambda_i^k$$

where λ_i are the (not necessarily unique) eigenvalues of \mathbf{A} . Without loss of generality, we assume that the eigenvalues are given in descending order, i.e. $\lambda_1 \geq \dots \geq \lambda_{|V|}$. Hence, an upper bound $\Delta^k(G) \leq |V|^2 \lambda_1^k$ can be derived based on the largest eigenvalue λ_1 of the adjacency matrix of G . We note that for the special case of a fully connected graph, where $\mathbf{A} = \mathbf{J}$, we have $\Delta^k(G) = \text{tr}(\mathbf{J}\mathbf{A}^k) = \text{tr}(\mathbf{J}^{k+1}) = \lambda_1^{k+1} = |V|^{k+1}$ and we thus recover the trivial case from above. \square

A.3 Synthetic data

In Section 4, we briefly described a model that generates pathways with injected correlation patterns, but could not include the pseudocode due to space constraints. Algorithm 3 presents pseudocode for constructing the graph topology, and Algorithm 4 shows how we generate a walk on this topology.

Algorithm 3 SyntheticModel(N, p, f, k): *Generates a directed $G_{N,p}$ graph and marks fraction f of length k pathways through G anomalous.*

Input: N (number of nodes), p (connection probability), f (fraction of anomalous pathways), k (anomaly order)
Output: G (weighted topology), paths (paths marked anomalous)

- 1: $G \leftarrow \text{directedER}(N, p)$
- 2: **for** $(i, j) \in G$ **do**
- 3: $G_{i,j} \leftarrow \text{unif}(1, 20)$ # Assign edge weight
- 4: $G^k \leftarrow \text{DeBruijnGraph}(G, k)$
- 5: anom-paths = \emptyset
- 6: **for** path $\in G^k$ **do**
- 7: **if** $\text{random}() < f$ **then**
- 8: anom-paths \leftarrow path # mark path anomalous
- 9: **return** G , anom-paths

Algorithm 4 SyntheticWalk(G, paths, l): Given a weighted first-order topology G and list of anomalous paths, generate a (potentially anomalous) random walk of length l .

Input: G (weighted network topology), paths (paths through G marked anomalous), l (length of walk)

Output: path

```

1:  $u \leftarrow$  uniform random node
2: path = [ $u$ ]
3: while  $j < l$  do
4:   if  $u$  is on an anomalous path then
5:     while  $j < l$  and nodes remain on anomalous path do
6:        $v \leftarrow$  next node on anomalous path
7:       Append  $v$  to path
8:        $j \leftarrow j + 1$ 
9:   else
10:     $v \leftarrow v \in N_u$  #  $\Pr(u, v) \propto$  edge weight  $G_{u,v}$ 
11:    Append  $v$  to path
12:     $j \leftarrow j + 1$ 
13:     $u = v$ 
14: return path

```

A.4 ROC Curves used to compute AUC

In Fig. 3, we presented area under the curve results for a binary classification experiment where we used HYPAs to predict ground truth over- and under-represented paths. In this section, we clarify the procedure for generating these results.

First, we use Algorithms 3 and 4 to generate a dataset with injected anomalies at order l . Then, for each value of k , we compute HYPAs^(k) scores, and for increasing α from 0 (nothing detected) to 1 (everything predicted as significant), we threshold the HYPAs^(k) scores to classify the ground truth over- and under-represented paths. We compute the true and false positive rates for each α , which results in a single ROC, where each point is a combination of k and α . We get an ROC for every combination of HYPAs order (k) and anomaly order (l). Finally, we compute the area under these curves and report averages and standard deviations over many randomly generated datasets, which is what is reported in Fig. 3.

A.5 Naive Baseline Method

Here we provide pseudocode for the Frequency Based Anomaly Detection (FBAD) method.

Algorithm 5 FBAD(S, k, α): Given path data S , order k , and scaling factor $\alpha \in \mathbb{R}$, compute anomalies based on the distribution of order- k edgeweights.

Input: S (input path data), k (desired anomaly order), α (scaling factor)

Output: G (k -th order network with anomaly-labeled transitions)

```

1:  $G \leftarrow$  DeBruijnGraph( $S, k$ )
2:  $\mu \leftarrow$  average of edge weights in  $G$ 
3:  $\sigma \leftarrow$  standard deviation of edge weights in  $G$ 
4: for edge  $e$  in  $G$  do
5:   if frequency( $e$ )  $> \mu + \sigma\alpha$  then
6:     Label  $e$  over-represented
7:   else if frequency( $e$ )  $< \mu - \sigma\alpha$  then
8:     Label  $e$  under-represented
9: return Labeled graph  $G$ 

```

A.6 Data

In Table 1 we presented some statistics of our datasets. Below we provide more detail about the specifics of how each dataset was constructed and processed before our analysis.

Tube. The Tube data is given in the form of origin-destination statistics between stations [22]. We then use these statistics in conjunction with the first-order topology of the Tube network to construct pathways by computing the shortest path between each origin and destination, then assuming riders take this path. If there are multiple shortest paths between an origin and a destination, the observed paths are distributed across them.

Journal Citations. The journal citation data begins with a citation graph [26], where a directed link is drawn from paper i to paper j if i cites j . We then enforce that this graph is directed and acyclic by removing “backlinks”, meaning links from node i to j such that j was published after i . Pathways of citations are then constructed by walking from a “source” paper (a paper which was never cited in the dataset) to a “sink” paper (a paper that didn’t cite any other papers in the dataset). Reversing the order of this pathway results in a chronological “citation flow” from the sink (the oldest paper) to the source (the newest paper). These sequences of papers are then projected using a mapping from individual paper to publication venue, giving us sequences of journals that cited one another through time. Our analysis is of this projected data.

Flights. The flights dataset is given in the form of “itineraries”, which correspond to tickets purchased together by a particular customer [48]. Each pathway is a sequence of airports corresponding to source, layovers, and destination. Our dataset is constructed by taking a uniform 5% sample of these pathways from the first quarter of 2018.

Hospital. The Sociopatterns data is a sequence of time stamped edges representing interactions between nurses, doctors, administrative staff and patients in a hospital [49]. We define a pathway by a 20-second inter-event time, meaning that if 2 interactions including a common person happened within 20 seconds, they are combined into a path. A path ends when 20 seconds passes without the last person to interact having a subsequent interaction.

Wikipedia. We focus our analysis of the Wikipedia data [51] on the pathways which represent finished games. In the full dataset, the number of observed pathways is too small relative to the size and density of the underlying article graph to compute meaningful statistics across the entire network. Due to this, we only analyze games which traverse the 100 most frequently visited articles in the dataset, and filter out pathways of length less than 4.

A.7 Simulation-based Labelling of Ground Truth Anomalies in Empirical Data

To evaluate the performance of our path anomaly detection method in section 4.1, we use numerical simulations to generate the expected empirical frequency distributions of all paths of length k in an empirical data set. We achieve this by randomizing an empirical data set by performing a large number of $(k - 1)$ -order random walks, where the length of random walks matches the lengths of

paths in the data set. For multiple randomizations of the data, we obtain expected frequency distributions of all paths of length k . Since computing the difference between actual and expected frequency (as in Fig. 2(c)) does not give us a notion of significance, we sample multiple randomized path datasets and maintain a list of observed frequencies for each transition. We use these random observations to estimate a multinomial distribution for the weight on each transition. We then compute the Cumulative Distribution Function of this estimated distribution and filter the transitions using a discrimination threshold in the same way as in HYP A. Based on this filtering, we obtain a ground truth against which we can compare HYP A and FBAD.

We note that in this analysis the construction of ground truth is dependent on the estimate of the multinomial distribution on each pathway, which in turn depends on the number of random datasets sampled (m in Algorithm 6). Due to the computational cost of simulating the more than 4 million random walks in the Tube dataset, in these experiments the estimated multinomial was constructed using only 2 observations.

Here we provide pseudocode for the construction of ground truth path anomalies given a pathway dataset. Note that the results in Fig. 4 are impacted by the sampling parameter m : as m increases, the discovered ground truth will get more accurate and the higher AUC will be for HYP A. An implementation of our numerical technique

to infer ground truth path anomalies will be made available upon publication of the paper [7].

Algorithm 6 GroundTruth(S, k, α, m): Given path data S , order k , discrimination threshold $\alpha \in \mathbb{R}$, and number of samples m , compute ground truth path anomalies based by numerical simulations.

Input: S (input path data), k (desired order), α (discrimination threshold), m (number of datasets to simulate)

Output: G (k -th order network with anomaly-labeled transitions)

```

1:  $G^{k-1} \leftarrow \text{DeBruijnGraph}(S, k-1)$ 
2:  $G^k \leftarrow \text{DeBruijnGraph}(S, k)$ 
3: for  $m$  simulations do
4:    $S_{\text{rnd}} \leftarrow \text{RandomWalks}(G^{k-1}, S)$ 
5:   Append frequency of each  $k$ th-order transition  $e \in G^k$  to list
6: for edge  $e$  in  $G^k$  do
7:   Estimate multinomial of  $e$ 's edgeweight  $w$  as  $\frac{x_w}{\sum_k x_w}$ 
8:   Compute CDF of multinomial distribution
9:   if  $\text{CDF}(e) \geq 1 - \alpha$  then
10:    Label  $e$  over-represented
11:   else if  $\text{CDF}(e) < \alpha$  then
12:    Label  $e$  under-represented
13: return Labeled graph  $G^k$ 

```
